Mon. Not. R. Astron. Soc. **000**, 000–000 (0000) Printed 7 December 2016 (MN LATEX style file v2.2)

Transit Probabilities Around Hypervelocity and Runaway Stars

G. Fragione[1⋆] and I. Ginsburg[2]
[1]*Department of Physics, Sapienza, University of Rome, P.le A. Moro 2, Roma, Italy*
[2]*Astronomy Department, Harvard University, 60 Garden St., Cambridge, MA 02138, USA*

arXiv:1609.03905v2 [astro-ph.EP] 6 Dec 2016

7 December 2016

ABSTRACT

In the blooming field of exoplanetary science, NASA's *Kepler Space Telescope* has revolutionized our understanding of exoplanets. *Kepler*'s very precise and long-duration photometry is ideal for detecting planetary transits around Sun-like stars. The forthcoming *Transiting Exoplanet Survey Satellite (TESS)* is expected to continue *Kepler*'s legacy. Along with transits, the Doppler technique remains an invaluable tool for discovering planets. The next generation of spectrographs, such as *G-CLEF*, promise precision radial velocity measurements. In this paper, we explore the possibility of detecting planets around hypervelocity and runaway stars, which should host a very compact system as consequence of their turbulent origin. We find that the probability of a multi-planetary transit is $10^{-3} \lesssim P \lesssim 10^{-1}$. We therefore need to observe $\sim 10 - 1000$ high-velocity stars to spot a transit. However, even if transits are rare around runaway and hypervelocity stars, the chances of detecting such planets using radial velocity surveys is high. We predict that the European *Gaia* satellite, along with *TESS* and the new-generation spectrographs *G-CLEF* and *ESPRESSO*, will spot planetary systems orbiting high-velocity stars.

Key words: planets and satellites: general – planets and satellites: detection – stars: planetary systems.

1 INTRODUCTION

Discoveries of exoplanets have proliferated in the past decade primarily due to observations with the Doppler technique and transits. Thanks to the high precision achieved with today's spectrographs, Doppler spectroscopy allows for the determination of a planet's minimum mass based upon the shift of stellar absorption lines. Cumming et al. (2008) analysed eight year's worth of radial velocity measurements for nearly 600 FGKM stars. The fundamental observational quantity is the stellar velocity amplitude induced by the planet (Cumming 2004; Cumming et al. 2008). Cumming et al. (2008) showed that 17-20% of stars have gas giant planets within 20 AU. Mayor et al. (2011) reported the results from an eight year survey using the HARPS spectrograph. They conclude that greater than half of solar-type stars harbour a planet with a period of $\leqslant$ 100 days. Furthermore, they find that $\sim$ 14% of solar-type stars host a planet with mass greater than 50 $M_\oplus$. Doppler observations are of vital importance and continue to help in discovering new planets (e.g. Dai et al. (2016)). However, today transits dominate the search for exoplanets.

A transit is the passage of a smaller body in front of a larger body, such as when an exoplanet passes in front of its host star thus producing a drop in brightness (Winn 2010). Several surveys have been dedicated to transits detections, the most important and fruitful of which is NASA's *Kepler Space Telescope*, which has revolutionized exoplanetary science (Borucki et al. 2010). *Kepler*'s original purpose was to determine the frequency and characteristics of planets and planetary systems in the habitable zone around FGKM stars. However, Kepler's very precise and long-duration photometry is ideal for detecting systems with multiple transiting planets (Lissauer et al. 2011b). NASA's next major exoplanet mission scheduled for launch in 2017 is the *Transiting Exoplanet Survey Satellite (TESS)*. *TESS* is expected to monitor several hundred thousand Sun-like stars for transiting planets across nearly the entire sky using four wide-field cameras (Ricker et al. 2015). *TESS* aims to combine the strengths of wide-field surveys with the fine photometric precision and long intervals of *Kepler*, but compared to Kepler will examine stars that are generally brighter by 3 mag over a solid angle that is larger by a factor of $\sim$ 400 (Sullivan et al. 2015). In this paper, we explore the possibility of detecting planets around high-velocity stars using both the Doppler technique and transits.

⋆ E-mail: giacomo.fragione@uniroma1.it

High-velocity stars are most often Galactic halo stars with high peculiar motions, usually divided in two different categories, runaway stars (RSs) and hypervelocity stars (HVSs). RSs are historically defined as Galactic young halo stars with peculiar motions higher than 40 km s^{-1}, which are thought to have travelled to the halo from their birthplace. RSs are produced in binary systems thanks to dynamical multi-body interactions or due to the velocity kick from a supernova explosion (Silva & Napiwotzki 2011). HVSs, on the other hand, are stars escaping the Galaxy. Hills (1988) was the first to predict the existence of HVSs, while Brown et al. (2005) discovered the first HVS in the outer halo. Hills' mechanism involves the tidal breakup of a binary passing close to a massive Black Hole (BH) (Ginsburg & Loeb 2006, 2007; Brown 2015; Fragione & Loeb 2016). Other mechanisms have, also, been proposed to explain the existence of HVSs, as the interaction of a massive binary black hole with a single star (Yu & Tremaine 2003), or the interaction of star clusters and BHs (Capuzzo-Dolcetta & Fragione 2015; Fragione & Capuzzo-Dolcetta 2016; Fragione, Capuzzo-Dolcetta & Kroupa 2016). Observations of high velocity and hypervelocity objects have usually been limited to high-mass, early-type, stars, due to observational bias (Brown, Geller & Kenyon 2014). However, recently observers have begun investigating low-mass HVSs candidates (Li et al. 2012; Palladino et al. 2014; Favia, West & Theissen 2015). The European Space Agency (ESA) satellite *Gaia* is expected to measure proper motions with an unprecedented precision, providing a larger and less biased sample ($\sim$ 100 new HVSs in a catalogue of $\sim 10^9$ stars). Moreover, *Gaia*'s sensitivity is good enough to search for multi-planet systems around massive stars and evolved stars and reveal their architecture and three-dimensional orbits (Casertano et al. 2008; Winn & Fabrycky 2015). Furthermore, the detection of a planet around a HVS or runaway star will provide valuable information on the survivability of planets in extreme environments (Ginsburg, Loeb & Wegner 2012).

Thus, in this paper we look at the likelihood of finding transits around such high-velocity stars. In Section 2 we discuss our approach to calculating transits including a discussion on the code we used. In Section 3 we explore various possibilities and discuss our outcomes. In Section 4 we explain additional difficulties that are inherent in observing multi-planet transits. In Section 5 we discuss the Doppler technique. We conclude with a discussion and implications for future observations in Section 6.

2 METHOD

The geometry of transits can be computed planet-by-planet only when dealing with planets independently (Murray & Correia 2010). When multi-planet systems are considered, the geometry becomes more complicated and has to be correctly understood in order to infer information on the architecture of such systems. Moreover, the ideal geometrical case does not provide a correct value for the transit probability because it fails to account for non-Keplerian orbits, duty cycles and signal-to-noise ratios (Brakensiek & Ragozzine 2016).

The geometric probability of a transit of a single planet (Murray & Correia 2010; Winn 2010) is given by

$$p_T = \frac{R_* \pm R_p}{a} \frac{1 + e \sin \omega}{1 - e^2}, \quad (1)$$

and depends on the star and planet radius (R_* and R_p respectively), the planet's orbital eccentricity (e), and the argument of periapsis (ω). The "+" sign allows grazing eclipses, while the "-" sign excludes them. In the case that $R_p \ll R_*$, and marginalizing over ω, the probability is simply

$$p_T \approx \frac{R_*}{a(1-e^2)} \approx 0.005 \left(\frac{R_*}{\mathrm{R}_\odot}\right) \left(\frac{1 \text{ AU}}{a}\right) \left(\frac{1}{1-e^2}\right) \quad (2)$$

A natural question is: how many systems do we need to observe to spot a transit? Once the planetary orbital distance is determined, we have to observe (Winn 2010)

$$N \gtrsim (\eta \, p_T)^{-1} \quad (3)$$

stars, where η is the fraction of stars that are thought to host such planets.

While the geometry of a single planet transit allows for an analytical calculation, there is no analytical solution for the transit probability of M planets. Furthermore, observations have shown that multi-planet systems are likely common. Lissauer et al. (2014) and Rowe et al. (2014) determined that approximately 40% of *Kepler*'s candidate are in multi-planet systems. Some of those systems are very compact. For example, Lissauer et al. (2011a) presented Kepler-11, a single Sun-like star with six transiting planets. Five of those planets have orbital periods between $\sim$ 10 and $\sim$ 47 days. Lissauer et al. (2012) studied the planetary system Kepler-33. In this system there are five transiting planets with periods ranging from around 5 to $\sim$ 41 days. Precise Doppler measurements have also revealed very compact systems. As an example, GJ 876 (Marcy et al. 2001; Riviera et al. 2010) is a red dwarf with four planets orbiting the star with semi-major axis between $\sim$ 0.02 AU and $\sim$ 0.33 AU. As pointed out by Lissauer et al. (2012), the vast majority of *Kepler*'s candidate multiple transiting systems are planets. The false positive rate being less than $\sim$ 1%. While in many instances it is safe to assume a single-planet system since the probability of detection is dominated by the innermost planet, clearly that is not appropriate in such compact systems and thus numerical techniques are required.

2.1 Multi-planet systems

In order to compute the transit probabilities for multi-planet systems we use the publicly available code CORBITS (Brakensiek & Ragozzine 2016). CORBITS is an algorithm that computes the combined geometric probability of a multi-transit in an exoplanetary system. The geometric probability of a transit is defined as the solid angle swept out by the planet's shadow on the celestial sphere. The transit region is defined as the union of all the shadowed star regions due to the planets' orbital motions. CORBITS is able to compute the surface area of any arbitrary intersection of these transit regions once supplied the star's radius R_* and the orbital elements a, e, i, ω, Ω (semi-major axis, eccentricity, inclination, argument of periapsis, and longitude of the

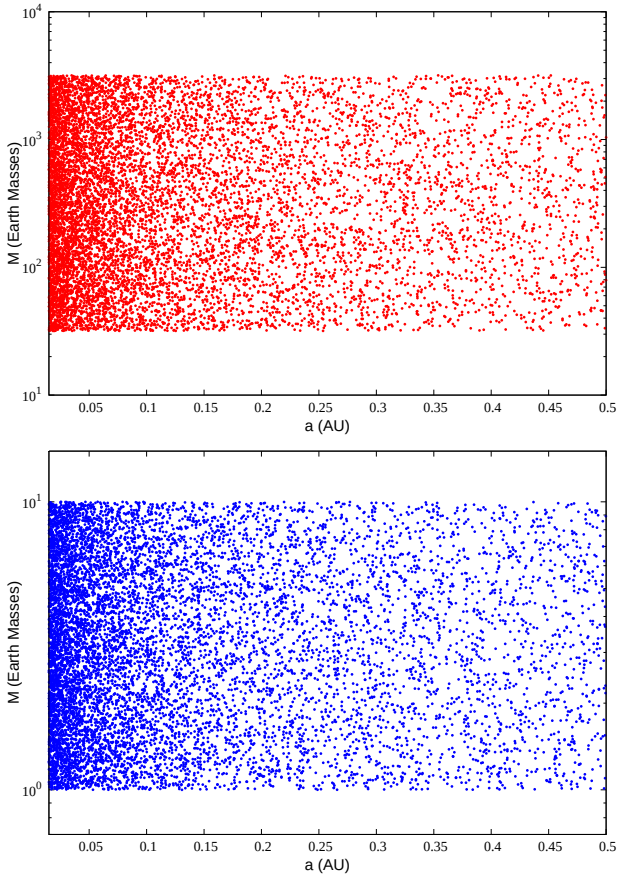

Figure 1. Planetary parameters (masses and semi-major axis) for high mass stars ($M_* > 1$ M$_\odot$, top panel) and low mass stars ($M_* \leqslant 1$ M$_\odot$, bottom panel).

ascending node respectively) of each planet. The code calculates the half-thickness $h_j = p_{T,j}$ (see Eq.2) for each planet, the geodesic curvature of each transit and, finally, thanks to the Gauss-Bonnet theorem, the joint probability of a multi-transit (Brakensiek & Ragozzine 2016). The code assumes fixed Keplerian orbits. The dynamical interactions between the planets alter the pure Keplerian orbit and the timing of the transits (Transit Timing Variation, TTV) (Agol et al. 2005; Holman & Murray 2005). However, such TTVs affect planetary phase, that are not relevant for p_T (Winn 2010), and modifications to the orbits are negligible on observational timescales (Brakensiek & Ragozzine 2016).

We choose the following set of initial conditions based upon Jurić & Tremaine (2008):

- Eccentricity generated according to a Rayleigh distribution with mean $0 \leqslant \sigma_e \leqslant 0.4$

$$f(e) = \frac{e}{\sigma_e} \exp\left(\frac{e^2}{\sigma_e}\right); \tag{4}$$

- Inclination generated according to a Rayleigh distribution with mean $0^\circ \leqslant \sigma_i \leqslant 40^\circ$

$$f(i) = \frac{i}{\sigma_i} \exp\left(\frac{i^2}{\sigma_i}\right); \tag{5}$$

- Semi-major axis generated according to a uniform distribution in $\log a$ with $0.015 \leqslant a/\mathrm{AU} \leqslant 0.5$;
- Period is computed using Kepler's Third Law

$$P = \frac{a(\mathrm{AU})^{1.5}}{\sqrt{M_*(\mathrm{M}_\odot)}} \text{ yr}; \tag{6}$$

- The argument of periapsis is generated according to a uniform distribution with $0^\circ \leqslant \omega \leqslant 360^\circ$;
- The longitude of the ascending node is generated according to a uniform distribution with $0^\circ \leqslant \Omega \leqslant 360^\circ$.

Although observed exoplanetary systems have small relative inclinations, and large mutual σ_i tend to make systems more dynamically unstable (Winn & Fabrycky 2015), we computed transits probabilities up to a mean inclination of 40°. We are primarily interested in systems that have undergone very strong gravitational interactions (Malmberg, Davies & Heggie 2011), as in the Hills mechanism that generates HVSs (Ginsburg, Loeb & Wegner 2012). For the same reason, the exoplanetary system needs to be compact in order that the star is able to retain its planets (Ginsburg et al. 2012). In order that the exoplanetary system is stable for enough time to be observable, the spacing of exoplanetary orbits has to satisfy the criterion (Chambers et al. 1996; Smith & Lissauer 2009; Lissauer et al. 2011b)

$$\frac{a_{i+1}}{a_i} = \frac{2(3M_*)^{1/3} + \beta(m_{i+1} + m_i)^{1/3}}{2(3M_*)^{1/3} - \beta(m_{i+1} + m_i)^{1/3}} \tag{7}$$

where a_i and m_i are the semi-major axis and mass of the i-th planet, respectively, and M_* is the host star mass. The lifetime of a planetary system generally decreases with increasing system multiplicity and planets masses and orbital eccentricities. However, the stability of a planetary system increases with the initial spacing measured in terms of β. β is a parameter that guarantees that the relative distance of two subsequent planets is big enough with respect to the mutual Hill radius

$$R_H = \left(\frac{m_{i+1} + m_i}{3M_*}\right)^{1/3} \frac{a_{i+1} + a_i}{2}. \tag{8}$$

Chambers et al. (1996) suggested that $\beta \gtrsim 10$ for $M > 3$ planets ensures the planetary stability over Gyrs. Smith & Lissauer (2009) determined that a spacing of $\beta \gtrsim 8$ is sufficient for Myr stability in systems with $M > 5$ equal mass planets. In our calculation, we set $\beta = 10$. The calculation of the Hill stability needs an assumption on planetary mass and radius. We generate planets masses according to a uniform distribution in $\log M_p$ (Jurić & Tremaine 2008) in the range $0.1 \leqslant M_p/\mathrm{M_J} \leqslant 10$ for $M_* > 1$ M$_\odot$. Figure 1 (top panel) illustrates the planets masses and orbital semi-major axis used in this paper for $M_* > 1$ M$_\odot$ stars. For low-mass stars ($M_* \leqslant 1$ M$_\odot$), we prefer the range $1 \leqslant M_p/\mathrm{M}_\oplus \leqslant 10$ for two reasons. First, the transit probabilities computed by CORBITS assumes that $R_* \gg R_p$, which is not true for $M_* \leqslant 1$ M$_\odot$ if $0.1 \leqslant M_p/\mathrm{M_J} \leqslant 10$. Second, *Kepler* observations suggest that there is a prevalence of Earth-sized planets around Sun-like stars (Petigura et al. 2013; Burke et al. 2015; Gaidos et al. 2016). However, the choice of two mass intervals for exoplanets is just to consider realistic systems spaced accordingly the Hill's criterion, since the transit is independent on the planets radii, but $p_T \propto a^{-1}$ (see Eq.2). Figure 1 (bottom panel) illustrates the planets masses and orbital semi-major axis used in this paper for $M_* \leqslant 1$ M$_\odot$

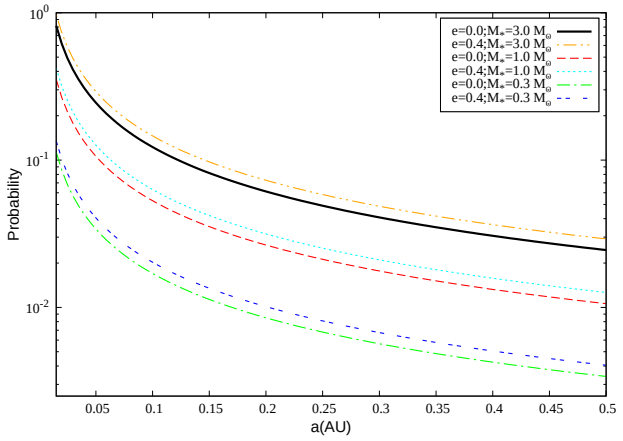

Figure 2. Transit probabilities for an exoplanet orbiting a host star of mass $M_* = 0.3$-1.0-3.0 $M_\odot$ as function of the orbital semi-major axis a.

stars. The mass range is important when dealing with the possibility of spotting real transits (see Section 4). When we generate the semi-major axis, it is accepted assuming it satisfies the above stability criterion; otherwise it is sampled again from the distribution.

3 GEOMETRICAL TRANSITS

The geometry of transits can be computed analytically by means of Eq.2 when dealing with stars that host a single exoplanet (Murray & Correia 2010; Winn 2010). Figure 2 illustrates the transit probabilities for an exoplanet orbiting a star of mass $M_* = 0.3$-3.0 $M_\odot$ as function of the orbital semi-major axis and eccentricity. The transit probability decreases as the orbital semi-major axis increases and is $10^{-3} \lesssim p_T \lesssim 1$. Moreover, the probabilities tend to be an increasing function of e and of the stellar mass M_* ($R_* \propto M_*^\beta$ with $\beta > 1$, see below) since Eq.2 is sensitive to high eccentricities and stellar radii. HVSs in the MMT survey are probably all main sequence $2.5-4$ $M_\odot$ B stars based on stellar rotation (Brown et al. 2014). Figure 2 shows that such massive stars yields large probabilities to planetary transits, which suggests that, if $\eta \sim 1$, about 50 HVSs should be observed to spot a transit. The present sample of ~ 20 HVSs gives a probability of observing a transit ~ 0.4. Although massive stars lead to larger probabilities, a transit must take into account the relative flux decrement $\sim (R_p/R_*)^2$. For example, if $M_* = 3.0$ $M_\odot$ it is possible that the star's luminosity would be overwhelming and thus a given telescope may not be sensitive enough to measure the drop in brightness (see Section 4).

In the case of a multi-planetary system, given the initial conditions discussed in the previous section, we compute the transit probabilities with CORBITS. We consider different star masses M_*, number of planets N_P, mean planetary inclinations σ_i and eccentricities σ_e. Each point in the figures (3, 4, and 5) is the average of 10^4 probabilities. Figure 3 shows the transit probabilities for an exoplanetary system orbiting a star of mass $M_* = 3.0$ $M_\odot$ as a function of the mean orbital eccentricity and inclination. We vary the number of planets from 2 (top panel), 3 (central panel) and 4 (bottom panel). Observed exoplanetary systems have small σ_i since large mutual inclination tends to make systems dynamically unstable (Winn & Fabrycky 2015). However, we computed transits probabilities up to $\sigma_i = 40^\circ$ since the planetary system can be highly perturbed after strong gravitational encounters (Malmberg et al. 2011; Ginsburg et al. 2012). The same reason leads us to consider very compact systems ($0.015 \leqslant a/\mathrm{AU} \leqslant 0.5$) (Ginsburg et al. 2012). The probability P_T is a decreasing function of the mean inclination. Detecting all of the planets in multi-planet systems becomes unlikely even when mutual inclinations are $\lesssim 1^\circ$ (Brakensiek & Ragozzine 2016). This illustrates one weak point in the transit method which is that from our perspective the planetary orbits need to line up with the star (Lissauer et al. 2011b; Brakensiek & Ragozzine 2016). However, probabilities tend to be an increasing function of σ_e since Eq.2 is sensitive to high eccentricities.

The joint probability of a multi-planetary transit is $10^{-3} \lesssim P_T \lesssim 10^{-1}$ and depends upon the semi-major axis range with $p_T \propto a^{-1}$. Equation 3 is indicative of the number of systems we have to observe to spot a transit. If we assume that all the stars in our sample host such planetary systems, $\eta \sim 1$. Given the computed probabilities, we need to observe $\sim 10 - 1000$ stars to spot a multi-planetary transit. Here, we are considering only the geometrical probability which is larger then the real probability because of duty cycles and signal-to-noise (S/N) ratios (see Section 4). As discussed, HVSs in the MMT survey are probably main sequence $2.5-4$ $M_\odot$ B stars (Brown et al. 2014). The present sample of ~ 20 HVSs gives a probability of observing a multi-planetary transit $\lesssim 0.2$ if $\eta \sim 1$. However, the *Gaia* satellite is expected to find ~ 100 HVSs in a catalogue of $\sim 10^9$ stars (Kenyon et al. 2014; Brown 2015; de Bruijne et al. 2015). Assuming each such HVS hosts a compact planetary system of at least 2 planets, Eq.3 predicts that at least one transit should be spotted.

Figure 3 also illustrates the behavior of the transit probabilities as a function of the different number of planets, N_P. As N_P increases, the probability of spotting a joint transit decreases. However, since the systems under consideration are constrained to be compact, and $p_T \propto a^{-1}$, the probability is $10^{-3} \lesssim P_T \lesssim 10^{-1}$, large enough to spot a system transiting one of the HVSs that are expected to be found with *Gaia*. There are two additional effects to be considered. First, due to their origin few stars are expected to host a large number of planets (Malmberg et al. 2011; Ginsburg et al. 2012). Even if the probability of spotting a transit of 4 planets is $\sim 10^{-3}$, few high velocity stars are expected to have survived with several planets ($\eta \ll 1$) and hence the real probability of transits falls dramatically. Second, if $\sigma_i > 0^\circ$, the transit probability can be smaller by an order of magnitude, or more for a higher number of planets. Systems with relative high inclinations are usually dynamically unstable, and observing a transit becomes quite difficult.

In our study, we have used a log-uniform distribution for the semi-major axis with $0.015 \leqslant a/\mathrm{AU} \leqslant 0.5$ (Jurić & Tremaine 2008). The details of the distribution function have important implications on the final joint probability. In order to investigate the effects of the semi-major axis distribution function, we computed transit probabilities sampling from different distributions. Figure 4 shows the ge-

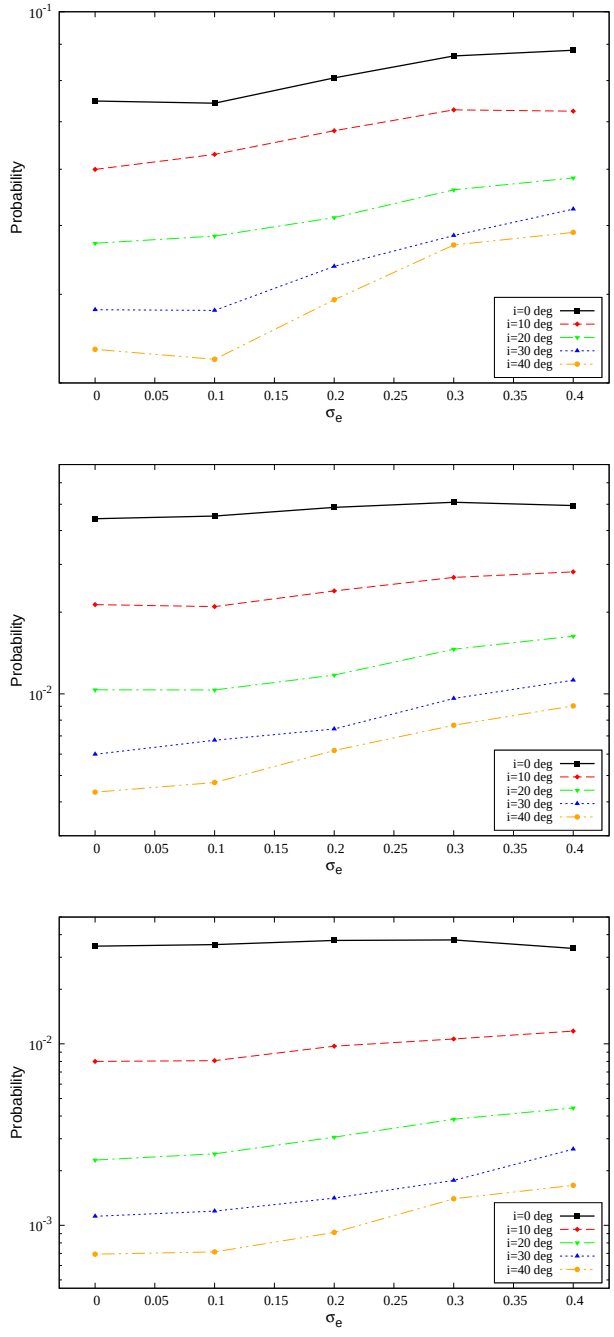

Figure 3. Transit probabilities for an exoplanetary system orbiting a host star of mass $M_* = 3.0$ $M_\odot$ as function of the mean eccentricity σ_e when the mean orbital inclination $0° \leqslant \sigma_i \leqslant 40°$. The number of planets varies from 2 (top panel), 3 (central panel) and 4 (bottom panel) planets.

ometrical probabilities for 2 planets orbiting a 3.0 $M_\odot$ star ($\sigma_i = 0°$), when the semi-major axis are sampled from a log-uniform distribution (black line), an exponential distribution with mean $\lambda^{-1} = 0.24$ AU (red line) and a uniform distribution (green line). Different semi-major axis distributions yield different geometrical probabilities, where the uniform distribution gives the lowest values. When sampling from that, large a, which yield to small P_T, have the same probability of small a, which yield to large P_T. On the contrary, the exponential distribution and the log-uniform distribution favor small semi-major axis, hence giving larger probabilities than the uniform distribution. However, the difference is just a factor of ~ 2. Similar results were obtained in the case that the 3.0 $M_\odot$ star hosts 3 or 4 planets. Furthermore, simulations by Ginsburg et al. (2012) show that the more compact a system, the more likely that system is to retain its planets after being disrupted. This suggests that a log-uniform or exponential distribution are well suited for our sampling.

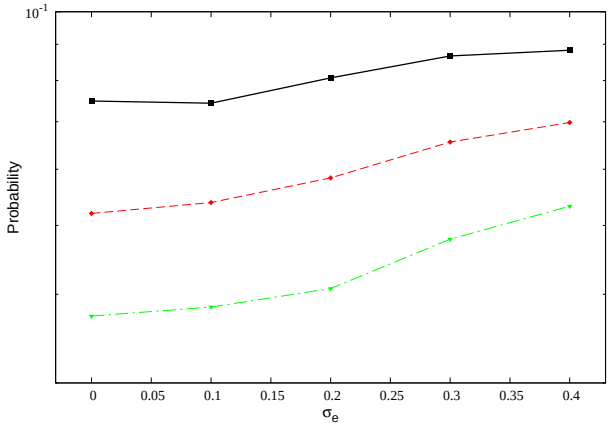

Figure 4. Transit probabilities for an exoplanetary system orbiting a host star of mass $M_* = 3.0$ $M_\odot$ as function of the mean eccentricity σ_e when the mean orbital inclination $\sigma_i = 0°$ and the star hosts 2 planets. The semi-major axis are sampled from a uniform distribution in $\log a$ (black line), an exponential distribution in a (red line) and a uniform distribution in a (green line).

Figure 5 shows the transit probabilities for an exoplanetary system orbiting a host star of mass 0.5 $M_\odot \leqslant M_* \leqslant 3.0$ $M_\odot$ as function of the mean eccentricity (σ_e) when the mean orbital inclination $\sigma_i = 0°$. We consider cases where the star hosts 2 (top panel), 3 (central panel), and 4 (bottom panel) planets. The probability P_T of a joint transit is an increasing function of the mass of the host star. Given the star's mass, we compute its radius from (Demircan & Kahraman 1991)

$$R_* = \begin{cases} 1.06\ M_*^{0.945} & M_* < 1.66\ M_\odot, \\ 1.33\ M_*^{0.555} & M_* > 1.66\ M_\odot. \end{cases} \quad (9)$$

Since $p_T \propto R_*$ and $R_* \propto M_*^\beta$, the geometrical probability of a transit increases with the star's mass. Even if massive stars lead to larger geometric probabilities, a transit must take into account the relative flux decrement $\sim (R_p/R_*)^2$, as discussed in the following section.

4 OBSERVING REAL TRANSITS

Once we determine that a transit has a reasonable geometric probability, we have to address the question whether such a transit can be detected. The additional combined effect of duty cycles and S/N ratios must be taken into consideration (Brakensiek & Ragozzine 2016).

The ratio Θ between the observing baseline of a telescope and the planets' orbital periods plays a fundamental role in detecting a transit. The transit duration of a single

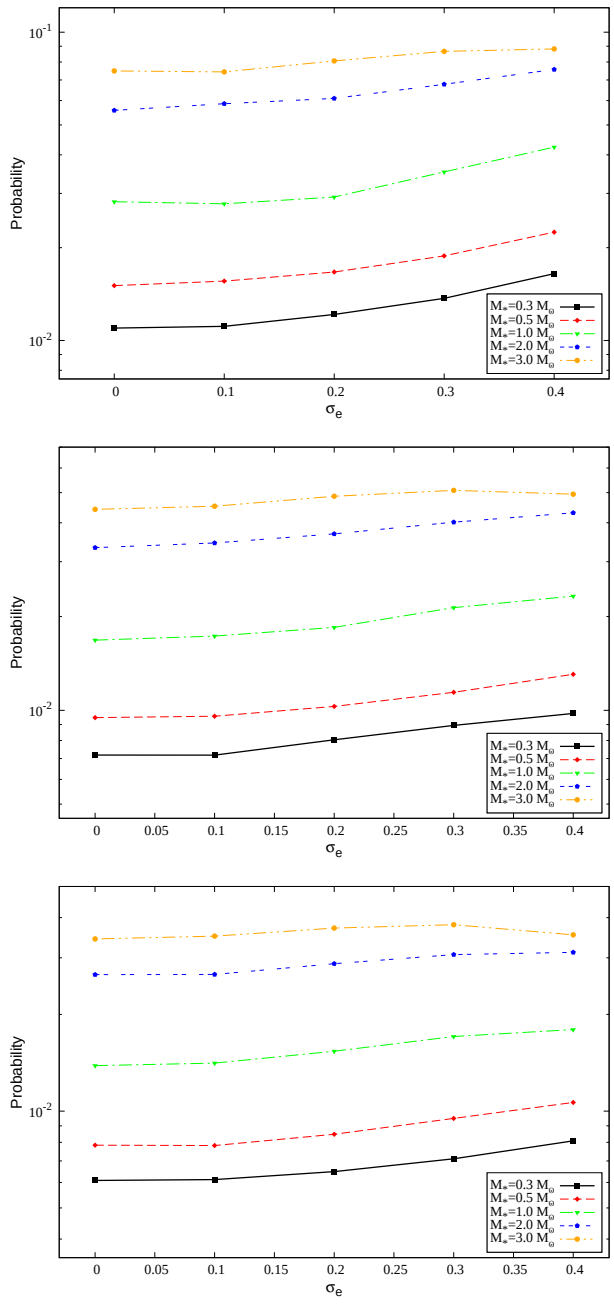

Figure 5. Planets transit probabilities for an exoplanetary system orbiting a host star of mass $0.5 \leqslant M_*/\mathrm{M}_\odot \leqslant 3.0$ as function of the mean eccentricity (σ_e) when the mean orbital inclination $\sigma_i = 0°$. We consider cases where the star hosts 2 (top panel), 3 (central panel), and 4 (bottom panel) planets.

planet (Winn 2010)

$$T = \left(\frac{R_* P}{\pi a}\sqrt{1-b^2}\right)\frac{\sqrt{1-e^2}}{1+e\sin\omega} \simeq 6\ \frac{P}{1\ \mathrm{day}}\frac{R_*}{a}\sqrt{1-e^2}\ \mathrm{hr} \tag{10}$$

depends on the impact parameter b, which is the minimum projected distance between the star and planet, expressed in units of the stellar radius (R_*), the exoplanet orbital eccentricity (e), the argument of periapsis (ω), and the period (P). If such a period is longer than the observing baseline, the probability of observing a single planet transit will become $p_{T,\theta} \approx p_T\Theta$. When dealing with multiple planets, the effect depends on the specific positions of the planets and the times of their observations. In this case it could be that $\Theta \ll 1$ and, even if the multi-transit has a reasonable geometric probability. Thus, we may be unable to observe such a transit.

To observe a transit, a photometric precision better than $\sim 1\%$ is needed (Beatty & Gaudi 2008). De facto this requirement implies that transits must be relatively nearby. *Kepler* has found planets orbiting stars out to a distance $\sim$ 2-3 kpc. However, to quantitatively estimate if a transit can be observed, it is necessary to compute the S/N ratio. Even when a transit occurs, and $p_{T,\theta}$ is high, it might not be detectable because of a low S/N ratio. The signal, i.e. the drop in brightness caused by the passage of planets, is proportional to the decrease in intensity (Winn 2010)

$$f(t) = \frac{F(t)}{F_*} = 1 + k^2\frac{I_p(t)}{I_*} - k^2\alpha_T \tag{11}$$

which depends on the disk-averaged intensities $I_p(t)$ and I_*, the conversion factor $k \propto R_p/R_*$, which is proportional to the ratio of the planet and stellar radii ($F_p/F_* = k^2 I_p(t)/I_*$), and the dimensionless function α_T, which depends on the overlap area between the stellar and planetary disks. The maximum loss of light is $f_{max} \simeq k^2 \propto R_p^2/R_*^2$. However, because of limb darkening, f_{max} is larger than k^2 when the planet is near the center of the star, and smaller than k^2 when the planet is near the limb. In any case, the computation of the S/N ratio for a transiting exoplanet is quite complicated, since one has to compute whether the transit would be detectable with specific transit-search pipelines (Fressin et al. 2013). We assume a simple formula for converting planets masses into radii (Lissauer et al. 2011b)

$$R_p = M_p(\mathrm{M}_\oplus)^{0.485}\ R_\oplus. \tag{12}$$

If we consider a Jupiter-sized planet and a HVS of typical mass 3 $\mathrm{M}_\odot$, the flux decrement is proportional to $k \propto (R_J/R_*)^2 \sim 0.1\%$. If the stellar mass is $\lesssim 1\ \mathrm{M}_\odot$, $k \sim 1\%$, while if the planet is Earth-sized, $k \lesssim 0.01\%$. Assuming that statistical correlation among data points from different transits are much weaker than among data points during the same transit, Pont et al. (2006) obtained

$$\mathrm{S/N} = \frac{\Delta * n}{\sqrt{\sum_{k=1}^{N_{tr}}\left[n_k^2\left(\frac{\sigma_w^2}{n_k}+\sigma_r^2\right)\right]}}, \tag{13}$$

where Δ is the transit depth in magnitudes, N_{tr} is the number of transits, n is the number of data points observed during all transits, n_k is the number of data points observed during the k-th transit, and σ_r and σ_w are the red and white noise in magnitudes, respectively. Whereas the white noise is uncorrelated from data point to data point, and typical sources are the photon and sky background noise, red noise is correlated from data point to data point and sources of red noise may be weather, seeing changes or intrinsic astrophysical changes in target brightness (Pont, Zucker & Queloz 2006; Von Braun, Kane & Ciardi 2009). The S/N ratio is thus a function of both the transit survey strategy and of astrophysical parameters. Given the above quantities, if S/N exceeds a certain threshold value, a transiting planet

is defined to be detectable in the data (Von Braun et al. 2009). Fressin et al. (2013) used $\chi = 7.1$ as threshold for the *Kepler* observations, while Sullivan et al. (2015) proposed a slightly larger threshold ($\chi = 7.3$) for *TESS* data. Even if detectable, the transit may not be observed. The window function determines the probability that a requisite number of transits required for detection occurs in the observational data, i.e. S/N transit exceeds this threshold, as a function of planetary orbital period (Burke et al. 2006; Von Braun et al. 2009; Burke & McCullough 2014; Burke et al. 2015). Beatty & Gaudi (2008) describe a general method to statistically calculate the number of transiting planets a given survey could detect. Calculating such transits is extremely complicated and often requires Monte-Carlo simulation. Such a treatment is beyond the scope of this paper. However, Burke et al. (2015) derived a simpler analytical expression of the form

$$\mathrm{S/N} = \sqrt{N_{tr}}\,\frac{\Delta}{\sigma}, \tag{14}$$

where $N_{tr} = M \times f_{duty} = (T_{obs}/P) \times f_{duty}$ is the expected number of transit events, σ is the detection noise, T_{obs} is the time baseline of observational coverage for a target and f_{duty} is the observing duty cycle, defined as the fraction of T_{obs} with valid observations. The probability of detection is defined as (Fressin et al. 2013; Burke et al. 2015)

$$P_{det} = \frac{1}{2} + \frac{1}{2}\,\mathrm{erf}\left(\frac{\mathrm{S/N} - 7.1}{\sqrt{2}}\right), \tag{15}$$

with a detection threshold of 7.1. Given that, 50% of transits with S/N = 7.1 are detected, while the detection probabilities are 2.3%, 15.9%, 84.1%, 97.7%, and 99.9% for S/Ns of 5.1, 6.1, 8.1, 9.1 and 10.1, respectively (Fressin et al. 2013). Assume for simplicity $\Delta \sim R_p^2/R_*^2$ and $N_{tr} \sim 1$, if $\sigma \sim 1\%$ the detection probabilities 2.3%, 15.9%, 84.1%, 97.7%, and 99.9% will correspond to $R_p/R_* \sim 0.23$, 0.25, 0.28, 0.30 and 0.32. Hence a Jupiter-sized planet transiting a 1 $M_\odot$ runaway star has $\gtrsim 90\%$ probability to be observed. On the other hand, if $\sigma \sim 10\%$, a 97.7% probability of detecting the transit implies that the host star and the planet have similar radii. When dealing with massive stars, such as the HVSs found by Brown et al. (2014), $\sigma \gtrsim 0.01$ since HVSs are brighter then solar mass stars and more distant (50 kpc $\lesssim d \lesssim$ 120 kpc). However, the S/N ratio can be significantly higher when dealing with the compact systems studied in the present work, since Δ will be the combination of the different $R_{p,i}^2/R_*^2$. Moreover, the *Gaia* mission will be able to spot ~ 100 HVSs within few kpc from the Sun and without restrictions in star mass. Hypervelocity and runaway candidates (Palladino et al. (2014), Favia et al. (2015), Li et al. (2012)) may host planetary transits that can be observed with a $> 50\%$ probability according to the previous discussion. Finally, as discussed, in order to determine the final probability of observing a transit, the window function must be taken into account (Von Braun et al. 2009; Burke et al. 2015). Burke & McCullough (2014) studied different window functions and found that planets with period $\lesssim 10$ days (as in the case of the planetary systems studied here) have a detection probability $\gtrsim 50\%$.

5 RADIAL VELOCITIES

Along with transits, the Doppler technique can help find planets around high-velocity stars. Radial Velocity (RV) surveys search for the variance in time of the Doppler shift of absorption lines in stellar spectra resulting from orbital motion of the stars due to an exoplanet (Clanton & Gaudi 2014). In order to detect a planet, the measurement uncertainties have to be low enough to distinguish the periodic variation of the signal. The typical uncertainty of the measurement of a stellar absorption line (Beatty & Gaudi 2015)

$$\sigma_{RV} \propto \frac{\Gamma^{3/2}}{W\ I_0^{1/2}} \tag{16}$$

depends on the FWHM of the absorption line Γ, its equivalent width W and the continuum intensity I_0. We are limited to luminous and nearby stars that have strong absorption lines and are bright enough to provide high S/N spectra (Stevens & Gaudi 2013).

The fundamental observational quantity in Doppler surveys is the stellar velocity amplitude induced by the planet (Cumming et al. 2008)

$$\begin{aligned} K &= \frac{28.4\ \mathrm{m/s}}{\sqrt{1-e^2}}\frac{M_p \sin i}{\mathrm{M_J}}\left(\frac{P}{1\ \mathrm{yr}}\right)^{-1/3}\left(\frac{M_*}{\mathrm{M_\odot}}\right)^{-2/3} = \\ &= \frac{28.4\ \mathrm{m/s}}{\sqrt{1-e^2}}\frac{M_p \sin i}{\mathrm{M_J}}\left(\frac{a}{1\ \mathrm{AU}}\right)^{-1/2}\left(\frac{M_*}{\mathrm{M_\odot}}\right)^{-1/2} \end{aligned} \tag{17}$$

where P is the orbital period, e is the eccentricity, M_* is the mass of the star, M_p is the mass of the planet and i is the orbital inclination. The S/N at which a RV survey can detect planets with a given period depends on the above stellar velocity amplitude, the magnitude of the measurement uncertainties σ, the total number of observations N_{RV} and the duration of the survey T_{RV} (Clanton & Gaudi 2014)

$$\begin{aligned} \mathrm{S/N} &\approx \left(\frac{N_{RV}}{2}\right)^{1/2}\left(\frac{K}{\sigma}\right) \\ &\times \left\{1 - \frac{1}{\pi^2}\left(\frac{P}{T_{RV}}\right)^2 \sin^2\left(\frac{\pi T_{RV}}{P}\right)\right\}^{1/2}, \end{aligned} \tag{18}$$

which, in the case $P \lesssim T_{RV}$, is well approximated by

$$\mathrm{S/N} \approx \left(\frac{N_{RV}}{2}\right)^{1/2}\left(\frac{K}{\sigma}\right). \tag{19}$$

Note that the above equation is nearly independent of the orbital period P. Given the above quantities, if S/N exceeds a certain threshold value χ_{RV}, a RV planet is detectable in the data. The typical threshold depends on the duration of the RV survey. Cumming (2004) showed that, in the case $P < T_{RV}$, the threshold for 50 per cent detection probability is

$$\chi^{50}_{RV,PT} = \frac{1}{\sqrt{N_{RV}}}\left[4\ln\left(\frac{M}{F}\right)\right]^{1/2}, \tag{20}$$

and for 99 per cent detection probability

$$\chi^{99}_{RV,PT} = 1.7\frac{1}{\sqrt{N_{RV}}}\left[4\ln\left(\frac{M}{F}\right)\right]^{1/2}. \tag{21}$$

On the other hand, in the case $P > T_{RV}$, the threshold for 50 per cent detection probability is

$$\chi^{50}_{RV,TP} = \frac{1}{\sqrt{N_{RV}}}\left[4\ln\left(\frac{M}{F}\right)\right]^{1/2}\left(\frac{2P}{\pi T_{RV}}\right), \tag{22}$$

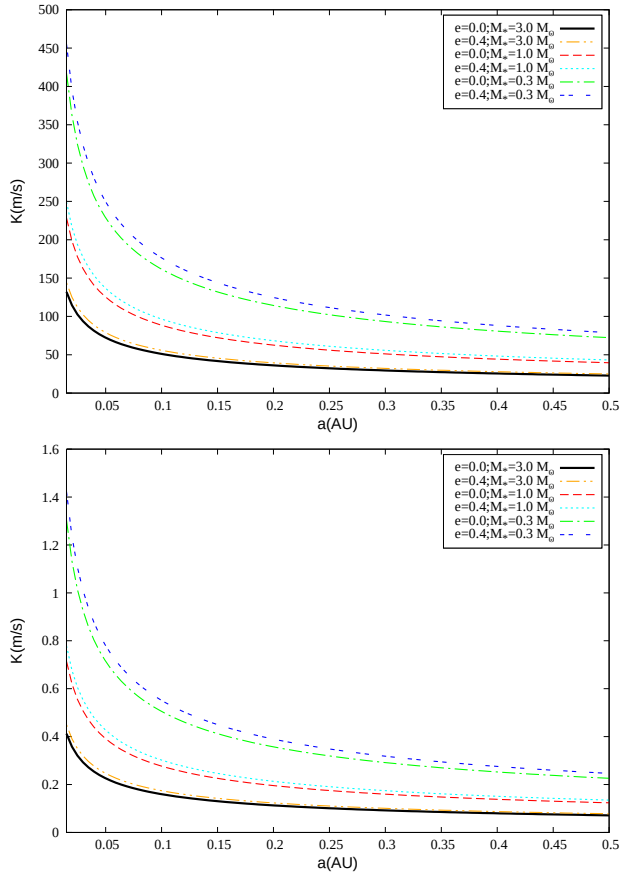

Figure 6. Stellar velocity amplitude induced by a planet of minimum mass 1 M_J (top panel) and 1 $M_\oplus$ (bottom panel) orbiting a host star of mass M_* = 0.3-1.0-3.0 $M_\odot$ as function of the orbital semi-major axis a.

and for 99 per cent detection probability

$$\chi^{99}_{RV,TP} = \frac{1}{\sqrt{N_{RV}}}\left[4\ln\left(\frac{M}{F}\right)\right]^{1/2}\left(\frac{2P}{\pi T_{RV}}\right)^2. \quad (23)$$

In the previous equations, M is the number of orbital frequencies ($2\pi/P_i$) that are used to describe the RV signal and F is the false alarm probability. M/F quantifies the significance of the Doppler signal due to an exoplanet based on how often a RV signal as large as the observed one would arise purely due to noise alone (Cumming 2004; Cumming et al. 2008). Typical values are $M/F \sim 10^6$ (Cumming 2004). In the case of eccentric orbits, thresholds are more complicated (Baluev 2015). However, Cumming (2004) reported that the eccentricity has an important effect when $e \gtrsim 0.6$, where the threshold can be one or two order of magnitude larger.

Figure 6 illustrates the stellar velocity amplitude induced by a planet of minimum mass $M_p \sin i = 1$ M_J (top panel) and $M_p \sin i = 1$ $M_\oplus$ (bottom panel) orbiting a host star of mass $M_* = 0.3$–3.0 $M_\odot$ as function of the orbital semi-major axis a. Figure 6 shows that the stellar velocity amplitude induced by the planet is $\sim$ 10-10^2 m s^{-1} for Jupiter-sized planets and of the order of unity for Earth-sized planets. The stellar velocity is also larger for smaller host stars and tight orbits, as consequence of Eq.17. Table 1 illustrates the typical values of the thresholds χ_{RV} as

Table 1. Thresholds for radial velocity surveys

N_{RV}	$\chi^{50}_{RV,PT}$	$\chi^{99}_{RV,PT}$	$\chi^{50}_{RV,TP}$	$\chi^{99}_{RV,TP}$
10	2.34	3.98	$1.50(P/T_{RV})$	$0.96(P/T_{RV})^2$
50	1.05	1.79	$0.67(P/T_{RV})$	$0.43(P/T_{RV})^2$
100	0.74	1.26	$0.47(P/T_{RV})$	$0.30(P/T_{RV})^2$

a function of the number of observations, N_{RV}. In the case $P > T_{RV}$, such values depend also on the ratio of the orbital period and of the survey duration.

Equations 18 and 19 give the typical S/N ratio for a Doppler signal due to an exoplanet. As discussed, RV surveys usually target luminous and nearby FGKM stars (Stevens & Gaudi 2013). Mayor et al. (2011) reported the results from an eight year survey using the HARPS spectrograph with typical radial velocity accuracy $\sigma \sim 1$ m s^{-1}. New-generation spectrographs, such as *G-CLEF* and *ESPRESSO*, are expected to have $\sigma \lesssim 50$ cm s^{-1}. Using such fiducial values and results from Fig.6, for a Jupiter-sized planet orbiting an FGKM star, S/N$\gtrsim 10^2$ well above the typical thresholds. On the other hand, Earth-sized planets have amplitudes, K, of the order of typical radial velocity accuracies and require long survey durations T_{RV} and large N_{RV}, in particular if they orbit massive stars. Cumming (2004) showed that very eccentric planets ($e \gtrsim 0.6$) have thresholds that can be one or two order of magnitude larger. In this case, the RV would require very large N_{RV}, in particular for Earth-sized planets. As discussed, hypervelocity and runaway candidates (Brown et al. (2014), Favia et al. (2015), Li et al. (2012)) may host compact planetary systems (Ginsburg et al. 2012), that can be observed with a $> 50\%$ probability according to the previous discussion. In particular, RV surveys can help to spot the Doppler signal due to planets more massive then Earth that orbit low-mass FGKM stars.

6 CONCLUSIONS

In this paper we have computed the likelihoods of finding exoplanets around high-velocity stars. We considered different stellar masses M_*, number of planets N_P, mean planetary inclinations σ_i and eccentricities σ_e. We found that the geometrical probability of detecting a transit has generally an increasing trend with σ_e as consequence of Eq.2, and decreases with σ_i. This indicates that the transit method may detect all of the planets in multi-planet systems if the planetary orbits are nearly lined up with the star (Lissauer et al. 2011b; Brakensiek & Ragozzine 2016). On the other hand, having a larger number of planets around less massive stars reduces the probability of spotting a transit.

We considered a semi-major axis in the range $0.015 \leqslant a/\mathrm{AU} \leqslant 0.5$ since the planetary system must be compact to be retained after strong gravitational encounters (Ginsburg et al. 2012). The joint probability of a multi-planetary transit is $10^{-3} \lesssim P \lesssim 10^{-1}$ and depends upon the semi-major axis range with $p_T \propto a^{-1}$. If we assume $\eta \sim 1$, Eq.3 predicts that we need to observe $\sim 10 - 1000$ stars to spot a transit. *TESS* is expected to spot transiting planets

across nearly the entire sky by monitoring several hundred thousand Sun-like stars (Sullivan et al. 2015). In particular, *TESS* should be able to find transits around hypervelocity and runaway stars. For HVSs, the *Gaia* satellite is expected to find ~ 100 such stars (Kenyon et al. 2014; Brown 2015; de Bruijne et al. 2015). If we assume that each HVS hosts a compact planetary system, Eq.3 predicts that at least one transit could be spotted.

Even if computations lead to larger geometric probabilities, a transit must take into account the relative flux decrement $(R_p/R_*)^2$ (Winn 2010). If we consider a Jupiter-sized planet and a HVS of typical mass 3 $M_\odot$, the flux decrement is proportional to $k \propto (R_J/R_*)^2 \sim 0.1\%$. If the star's mass is $\lesssim 1$ $M_\odot$, $k \sim 1\%$. While the geometrical probability favors heavier stars, the relative flux decrement indicates that the S/N ratio is larger in the case of small stars. Assuming $\sigma \sim 1\%$, a Jupiter-sized planet transiting a 1 $M_\odot$ star have $\gtrsim 90\%$ of probability to be observed. *Gaia* will spot ~ 100 HVSs within few kpc from the Sun. Transits are likely to be observed around such HVSs with $\gtrsim 90\%$ probability if they host planets.

Along with transits, the Doppler technique is an important tool for finding planets around high-velocity stars. Equation 17 indicates that the stellar velocity amplitude induced by the planet is $K \sim$ 10-10^2 m s^{-1}, with larger values for FGKM stars. The detection threshold depends on the number and duration of the observations and on the noise sources (Cumming et al. 2008). Generally the detection threshold is $\gtrsim 1$ m s^{-1}, and depends on the duration of the RV survey and on the planet's orbital period and eccentricity (Cumming 2004). The typical radial velocity accuracy ($\sigma \sim 1$ m s^{-1}) of modern spectrograph yield $> 50\%$ probability of measuring the Doppler shift caused by a hot-Jupiter, whereas Earth-sized planets require long survey durations and large number of observations. In general, compact planetary systems with large planetary minimum masses around low-mass stars can generate a high Doppler signal, that can be measured with $> 50\%$ probability by the next-generation spectrographs.

As discussed, transits are particularly suited for spotting Jupiter-sized exoplanets around low-mass high-velocity stars. On the other hand, RV surveys are able to observe not only massive planets, but also Earth-sized planets orbiting massive high-velocity stars provided that the duration of the survey is large enough and that the Doppler signal is measured several times. Thus, a combination of Doppler spectrographs, such as *G-CLEF* and *ESPRESSO*, working together with *TESS* will hopefully lead to the discovery of planets around high-velocity stars and consequently result in new understandings of planetary formation, evolution, and survivability.

ACKNOWLEDGMENTS

We thank Avi Loeb, Matt Holman, Dimitar Sasselov, Debra Fischer, and our anonymous referee for insightful comments on the paper. GF acknowledges hospitality from the Institute for Theory and Computation at the Harvard-Smithsonian Center for Astrophysics, where the early plan for this work was conceived. GF acknowledges Sapienza University of Rome for the grant "Progetti Avvio alla Ricerca" (Starting Research Grant, 0051276), which funded part of this work. IG was supported in part by funds from Harvard University and the Institute for Theory and Computation at the Harvard-Smithsonian Center for Astrophysics.

REFERENCES

Agol E., Steffen J., Sari R., Clarkson W., 2005, MNRAS, 359, 567
Baluev R.V., 2015, MNRAS, 446, 1478
Beatty T.G., Gaudi B.S., 2008, ApJ, 686, 1302
Beatty T.G., Gaudi B.S., 2015, PASP, 127, 1240
Borucki W.J. et al., 2010, Sci., 327.5968, 977
Brakensiek J., Ragozzine D., 2016, ApJ, 821.1, 47
Brown W.R., 2015, ARA&A, 53, 157
Brown W.R., Geller M.J., Kenyon S.J., 2014, ApJ, 787, 89
Brown W.R., Geller M.J., Kenyon S.J., Kurtz M.J., 2005, ApJ Lett., 622, L33
Burke C.J. et al., 2015, ApJ, 809, 8
Burke C.J., Gaudi B.S., DePoy D.L., Pogge R.W., 2006, AJ, 132, 210
Burke C.J., McCullough P.R., 2014, ApJ, 792, 79
Casertano S. et al., 2008, A& A, 482, 699
Clanton C., Gaudi B.S., 2014, ApJ, 791, 90
Cumming A. 2004, MNRAS, 354, 1165
Cumming A., Butler R.P., Marcy G.W., Vogt S.S., Wright J.T., Fischer D.A., 2008, PASP, 120, 531
Capuzzo-Dolcetta R., Fragione G., 2015, MNRAS, 454, 2677
Chambers J. E., Wetherill G.W., Boss A.P., 1996, Icarus, 119.2, 261
Dai F., Winn J.N. Albrecht S. et al., 2016, ApJ, 823, 115
de Bruijne J.H.J. et al., 2015, A& A, 576, A74
Demircan O., Kahraman G., 1991, Astrophys. Spa. Sci. 181, 313
Favia A., West A.A., Theissen C.A., 2015, ApJ, 813, 26
Fragione G., Capuzzo-Dolcetta R., 2016, MNRAS, 458, 2596
Fragione G., Capuzzo-Dolcetta R., Kroupa P., 2016, preprint (arXiv:1609.05305)
Fragione G., Loeb A., 2016, preprint (arXiv:1608.01517)
Fressin F. et al., 2013, ApJ, 766, 81.
Gaidos E., Mann A.W., Kraus A.L., Ireland M., 2016, MNRAS, 457, 2877
Ginsburg I., Loeb A., 2006, MNRAS, 368, 221
Ginsburg I., Loeb A., 2007, MNRAS, 376, 492
Ginsburg I., Loeb A., Wegner G.A., 2012, MNRAS ,423.1, 948
Hills J.G., 1988, Nature, 331, 687
Holman M.J., Murray N.W., 2005, Sci., 307, 1288
Jurić M., Tremaine S., 2008, ApJ, 686, 603
Kenyon S.J., Bromley B.C., Brown W.R., Geller M.J., 2014, ApJ, 793, 122
Li Y., Luo A., Zhao G., Lu Y., Ren J., Zuo F., 2012, ApJ Lett., 744, L24
Lissauer J.J., Marcy G.W., Bryson S.T. et al., 2014, ApJ, 784, 44
Lissauer J.J., Marcy G.W., Rowe J.F. et al., 2012, ApJ, 750, 112
Lissauer J.J., Fabrycky D.C., Ford E.B., Borucki W.J. et al., 2011a, Nature, 470, 53

Lissauer J.J., Ragozzine D. et al., 2011b, ApJ Suppl. Series 197.1, 8
Malmberg D., Davies M.B., Heggie D.C., 2011, MNRAS, 411, 859
Marcy G.W., Butler R.P., Fischer D. et al., 2001, ApJ, 556, 301
Mayor M. et al., 2011, preprint (arXiv:1109.2497)
Murray C., Correia A., 2010, Exoplanets. Arizona Univ. Press, Tucson, p. 15
Palladino L.E. et al., 2014, ApJ, 780, 7
Petigura E.A., Howard A.W., Marcy G.W., 2013, Proc. Natl. Acad. Sci., 110.48, 19273
Pont F., Zucker S., Queloz D., 2006, MNRAS, 373, 231
Silva M.D.V., Napiwotzki R., 2011, MNRAS, 411, 2596
Smith A.W., Lissauer J.J., 2009, Icarus, 201, 381
Sullivan P.W. et al., 2015, ApJ, 809, 77
Ricker G.R. et al., 2015, SPIE Jour. Astron. Telesc. Instrum. Syst., 1, 014003
Rivera E.J. et al., 2010, ApJ, 719, 890
Rowe J.F., Bryson S.T., Marcy G.W., Lissauer J.J. et al., 2014, ApJ, 784, 45
Stevens D.J., Gaudi B.S., 2013, PASP, 125, 933
Von Braun K., Kane S.R., Ciardi D.R., 2009, ApJ, 702, 779
Winn J.N., 2010, Exoplanet Transits and Occultations, ed. S. Seager, 5577
Winn J.N., Fabrycky D.C., 2015, Annu. Rev. Astron. Astrophys., 53, 409
Yu Q., Tremaine S., 2003, ApJ, 599, 1129